ARL-TR-7588 ● FEB 2016

US Army Research Laboratory

Ball-on-Disc Tribometer's Protocol Development: Loss of Lubrication Evaluation

by Mark R Riggs, Stephen P Berkebile, and Nikhil K Murthy

NOTICES

Disclaimers

ARL-TR-7588 ● FEB 2016

US Army Research Laboratory

Ball-on-Disc Tribometer's Protocol Development: Loss of Lubrication Evaluation

by Mark R Riggs and Stephen P Berkebile
Vehicle Technology Directorate, ARL

Nikhil K Murthy
Engility, Chantilly, Virginia

REPORT DOCUMENTATION PAGE

Form Approved
OMB No. 0704-0188

1. REPORT DATE *(DD-MM-YYYY)*	2. REPORT TYPE	3. DATES COVERED (From - To)
February 2016	Final	July 2014 to November 2015

4. TITLE AND SUBTITLE
Ball-on-Disc Tribometer's Protocol Development: Loss of Lubrication Evaluation

5a. CONTRACT NUMBER

5b. GRANT NUMBER

5c. PROGRAM ELEMENT NUMBER

6. AUTHOR(S)
Mark R Riggs, Stephen P Berkebile, and Nikhil K Murthy

5d. PROJECT NUMBER

5e. TASK NUMBER

5f. WORK UNIT NUMBER

7. PERFORMING ORGANIZATION NAME(S) AND ADDRESS(ES)
US Army Research Laboratory
ATTN: RDRL-VTP
Aberdeen Proving Ground, MD 21005-5066

8. PERFORMING ORGANIZATION REPORT NUMBER
ARL-TR-7588

9. SPONSORING/MONITORING AGENCY NAME(S) AND ADDRESS(ES)

10. SPONSOR/MONITOR'S ACRONYM(S)

11. SPONSOR/MONITOR'S REPORT NUMBER(S)

12. DISTRIBUTION/AVAILABILITY STATEMENT
Approved for public release; distribution is unlimited.

13. SUPPLEMENTARY NOTES

14. ABSTRACT
Loss of lubrication (LoL) protocol development consists of determining the proper parameters to simulate relevant gear-and-bearing contact conditions under starved lubrication. The goal is to evaluate the performance of materials and lubricants and ultimately improve the survivability of rotorcraft propulsion components under those starved-lubrication conditions. A ball-on-disc tribometer aids in discovering new solutions through experimentally simulating gear contacts at high-speed and high-load conditions with precise control over the operating conditions. These simulated gear contacts are used to investigate tribological properties of gear materials, surface finishes, coatings, and lubricants under starved-lubrication conditions. New materials that demonstrate superior performance during an LoL event are desirable to improve operational capabilities under severe lubrication conditions. This paper discusses a variety of methods to evaluate survivability and the development of an LoL-experiment protocol with a ball-on-disc tribometer. Study and experimentation of new oil-off protocols at the coupon level will contribute toward creating innovative solutions for an oil-off event with improved survivability to protect our Soldiers.

15. SUBJECT TERMS
starved, lubrication, protocol, evaluation, tribometer, loss of lubrication

16. SECURITY CLASSIFICATION OF:			17. LIMITATION OF ABSTRACT	18. NUMBER OF PAGES	19a. NAME OF RESPONSIBLE PERSON
					Mark R Riggs
a. REPORT	b. ABSTRACT	c. THIS PAGE			19b. TELEPHONE NUMBER (Include area code)
Unclassified	Unclassified	Unclassified	UU	32	410-278-9604

Contents

List of Figures

List of Tables

1. Introduction

Loss of lubrication (LoL) within a helicopter gear box can lead to critical failure modes because of oil starvation within meshing gears or bearings. The US Army's Aeronautical Design Standard (ADS)-50-PRF (in Subsection 5-4.3.5) requires an oil-out test for subsystem bench-testing qualification. Each transmission and gearbox configuration must be able to operate at flight conditions for 30 minutes (min) from the time the low-level warning system is activated for 2 test repetitions.[1]

Meeting the ADS-50-PRF requirement is challenging because metal-to-metal contact is experienced between the previously lubricated surfaces once the liquid lubricant film is gone and the remaining boundary film has been degraded. In a gear mesh, for example, heat generation is increased by frequent asperity interactions, and a reduced capacity to dissipate heat is caused by the decreased availability of oil to advect heat away from the mesh. The combination of heat generation and an inability to dissipate heat leads to a thermal runaway in the gear mesh. The thermal runaway causes local welding and tearing between gear teeth and plastic deformation of the gear teeth that results in a loss of tooth profiles and reduced torque transmission. The thermal and mechanical effects of an LoL event will continue to escalate until failure of the gearing system. The scenario is similar for bearings.

One example of a crash due to loss of lubrication occurred in March 2009 with a Sikorsky S-92 helicopter off the coast of Canada.[2] The Sikorsky's filter-bowl mounting studs fractured close to takeoff and allowed the oil to leak. The leak was severe enough to deplete the oil reservoir for the main gearbox and create a starved-lubrication condition. The helicopter's tail take-off pinion failed and caused a crash into the Atlantic Ocean with 18 passengers and crew aboard. The failed pinion is shown alongside an undamaged pinion in Fig. 1.

Fig. 1 The damaged pinion (right) from the Sikorsky S-92 that crashed in 2009 compared to a new pinion gear (left)[2]

There have been several efforts to study the LoL process. The Loss of Lubrication Rig at the National Aeronautics and Space Administration's (NASA's) Glenn Research Center in Cleveland, Ohio, is one example of a current research effort.[3] One set of experiments evaluated backup lubrication methods such as a fine oil mist or grease injection after the main oil supply is turned off.[3] Using a pair of gears, the results from NASA's rig give a holistic view of failure on a full component level; however, a precise indication of the failure initiation is also desirable. A method capable of measuring the initiation of mechanisms of failure aids in a fuller understanding of the failure process and in the creation of technologies for preventing failure. A ball-on-disc tribometer can offer such a method.

A ball-on-disc tribometer is capable of simulating gear contacts at high speed and high load with precise control over the operating conditions. Control of the vertical load, oil flow, oil and disc temperature, entrainment velocity, slip percentage, and geometric orientations enables the ball-on-disc tribometer to flexibly simulate gear and bearing contacts. The precise control allows a specific point of contact from the gear mesh to be evaluated. A particular point in the gear mesh also corresponds to specific points of the gear-tooth profile of the driving and driven gears. Protocols simulating contact conditions at specific locations along the tooth profile allow the researcher to clearly identify the initiation of mechanisms of failure.

The ball-on-disc tribometer is shown in Fig. 2, where the ball linear velocity (Ub) and disc linear velocity (Ud) are controlled with independent motors to create entrainment velocities (Ue) with controlled slip percentages. The entrainment velocity is defined as the average of the ball's and disc's linear velocities. The slip percentage is shown in Eq. 1. The ball thermocouple (Tb) and disc thermocouple (Td) give temperature readings of the specimen. Additional information regarding the ball-on-disc tribometer's working envelope and geometric construction are found in a 2015 report published by the US Army Research Laboratory (ARL).[4]

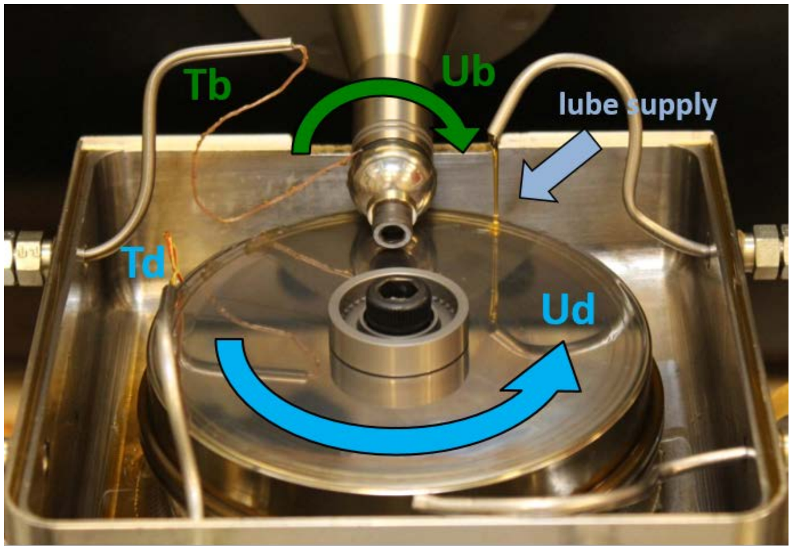

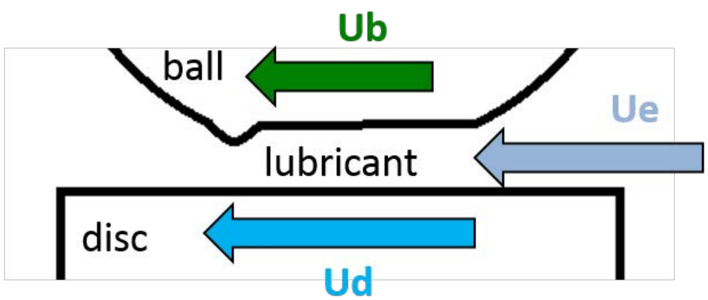

Fig. 2 Ball-on-disc tribometer

$$Slip\ Percentage\ (\%) = \frac{U_b - U_d}{U_e} * 100\% \qquad (1)$$

2. Protocol Development

The protocol used to evaluate gear-contact conditions with a ball-on-disc tribometer must produce controlled and repeatable contact conditions with a focused result. The entrainment velocity, slip percentage, load, and oil supply must be considered in order to evaluate the coupon material, surface finish, coating, and novel lubricants. Two protocols are described here: the load capacity (LC) protocol and the LoL protocol, which also is known as the oil-out (OO) protocol. The LC protocol is used as a screening procedure to compare the severity of contact conditions at interesting locations on the tooth profile. Once the most severe condition is identified, the LoL protocol is performed to measure the time to failure in a LoL condition.

2.1 Gear-Contact Conditions

The first step in creating a protocol for gear simulation is to identify which gear contacts need to be simulated. The gear set chosen for this preliminary protocol development was the set of NASA spur gears used in previous LoL experimentation at the component level to create coupon-level evaluations that directly relate to component-level evaluation capability within ARL.[3]

The spur gears have 2 main "severe" conditions within the gear-tooth profile. The first condition is called highest sliding (HS), when a gear tooth is entering or leaving contact, and the second is called single-tooth (ST) contact, when a single tooth begins to transfer the entire load rather than sharing the load between 2 teeth. The location on the tooth profile where the single-tooth contact begins represents the highest sliding velocity when only one tooth is bearing the load. The parameters for these conditions were based on the conditions found in the previous ARL report[4] for the NASA spur gears. The final parameters used for the protocol experiments to define each contact condition are shown below in Table 1. The relative-velocity vectors of the surfaces are parallel to one another because of the spur gear's geometry.

Table 1 NASA's spur gear contact-condition parameters

Condition	Entrainment velocity (m/s)	Slip percentage (%)	Load (N)	Hertzian contact stress (GPa)
HS	16	–100	100	1.29
ST	16	–23	200	1.63

2.2 LC Protocol

The LC experiment was originally designed by Wedeven Associates Inc., to screen advanced lubricant formulations as a replacement for the Ryder Gear Test Method.[5] The basic structure of the load-capacity protocol is to run at a constant contact velocity with the load increasing in a step-wise fashion until failure or until every load stage is completed up to a specified load. The LC experiment's stages are listed in Table 2. Before these load stages were implemented, a simpler stage sequence was used starting with 10 N and increasing by 10 N until 100 N. At 100 N the sequence changed to increase by 20 N until the last load stage at 600 N. The

Wedeven-developed, load-stage protocol increases the Hertzian contact stress in 3 regimes that are linear in calculated contact stress (Steps 1 and 2 and Steps 3–24 and 25–30) and also to the final load stage more rapidly than using the linear increase in force, as shown in Fig. 3.

Table 2 LC protocol's load stages

Load stage	Load (N)	Stress (GPa)
1	17.76	0.7273
2	28.86	0.8551
3	34.19	0.9048
4	41.51	0.9652
5	48.84	1.019
6	58.61	1.0828
7	68.38	1.14
8	78.14	1.1918
9	87.91	1.2395
10	100.12	1.2944
11	112.33	1.3451
12	124.54	1.3921
13	136.75	1.4362
14	151.4	1.4858
15	166.06	1.5323
16	180.71	1.5761
17	195.36	1.6175
18	212.45	1.6634
19	229.55	1.7069
20	246.64	1.7482
21	263.74	1.7877
22	285.94	1.8365
23	312.57	1.8919
24	343.66	1.9526
25	379.18	2.0177
26	419.14	2.0862
27	463.54	2.1574
28	512.38	2.2307
29	565.66	2.3055
30	621.6	2.3791

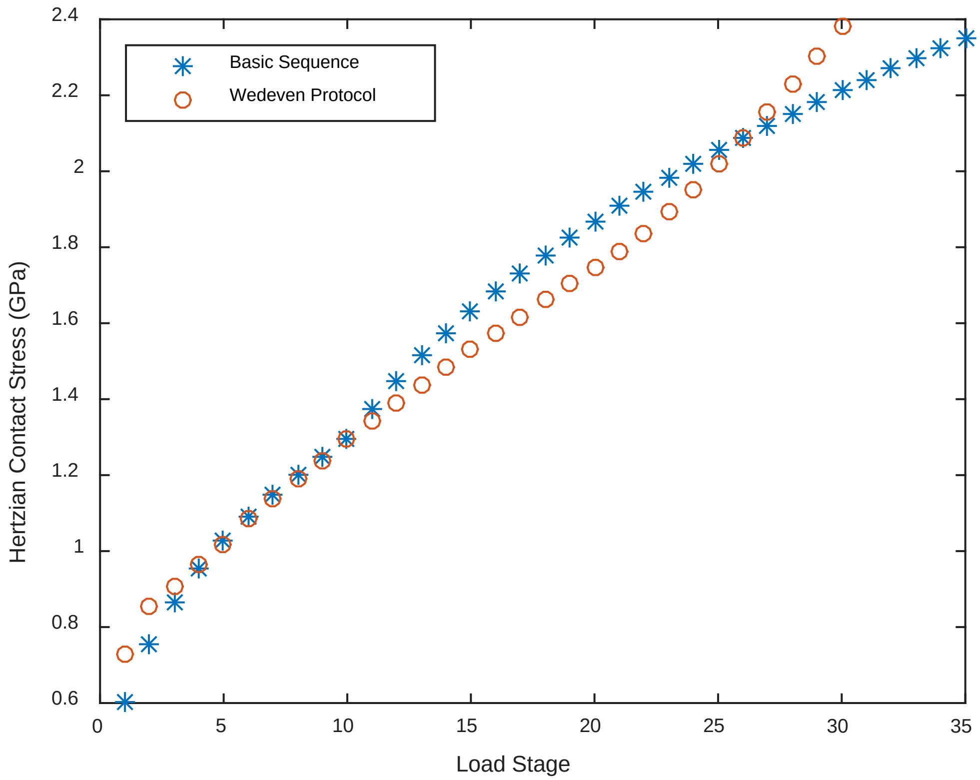

Fig. 3 Resultant Hertzian contact plot for the load-stage protocols

To keep the LC experiments consistent, a fully flooded oil supply is delivered at 126 °C. The disc is also heated to 126 °C and both temperature are maintained ±10 °C. The experiment is stopped once the traction coefficient reaches 0.15, which indicates failure of the remaining oil and boundary-layer films and the onset of scuffing. The material, surface finish, oil, and other specimen-related properties can be varied to determine the relative performance for load-carrying capacity. The materials used for the LC protocol's development were 9310 alloy steel with as-ground surfaces and Mobil Jet II (MJII) oil to determine which of the 2 contact conditions, highest sliding or single tooth, is the more severe. The as-ground surfaces do not have additional polishing or surface treatment other than the circumferential grinding process leading to a roughness average, Ra, value of 0.17 µm. Other than load, the contact conditions used for LC evaluation were chosen to represent the NASA spur gears (as listed previously in Table 1). For the load, both the constant steps and the steadily increasing step sequences were used.

2.2.1 Oil-Supply Challenges

The basic setup for the ball-on-disc tribometer uses an oil-dispersion ring, also called an oil slinger. The concept of the oil slinger is to evenly distribute a thin film of oil across the surface of the disc from a single oil source, which is driven by a peristaltic pump. Figure 4a shows the oil-delivery setup in a Wedeven Associates Machine (WAM). The slinger contains small holes around the outer diameter, which is also raised from the disc's surface with a 0.007-inch undercut (as shown in Fig. 5). This undercut allows the oil to drip onto the surface of the disc. This process works well for relatively low disc speeds, but unwanted oil behaviors emerge once the disc speed is increased. The flash-photography image in Fig. 4b shows oil wicking up the lower outer edge of the oil slinger and releasing from its undercut surface in small droplets. These droplets fly out radially from the center above the surface of the disc and fail to lubricate the surface. The most effective way to create a flooded contact in high-disc-speed conditions is to pump a steady oil supply directly in front of the ball-and-disc contact, as shown in Figure 4c. Supplying oil at a controlled rate to create a starved-lubrication behavior is challenging at high speeds because not all of the oil wets the surface of the disc, as shown in Fig. 4d.

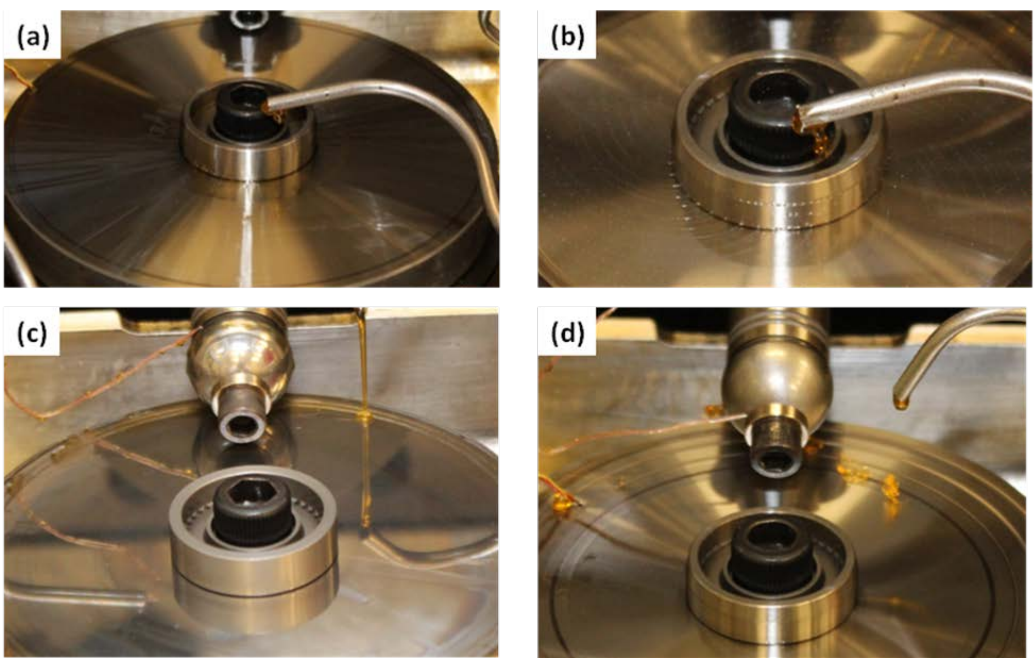

Fig. 4 WAM oil-delivery challenges

Fig. 5 Oil slinger

The behavior of the oil film while using the oil slinger was qualitatively compared across a matrix of disc temperatures, pump speeds, and disc speeds. Each matrix value was photographed and analyzed to see when oil droplets began to separate from the disc. The matrix parameters and results are shown in Table 3.

Table 3 Oil-slinger analysis of oil-droplet-formation parameters

	Temperature 20 °C			Temperature 80 °C			Disc 126 °C, Oil 80 °C	
Oil-pump speed (ml/min) / **Disc speed (rpm)**	**2.5**	**7.6**	**12.2**	**2.5**	**7.6**	**12.2**	**2.5**	**12.2**
200	. . .	. . .	. . .	. . .	. . .	. . .	. . .	. . .
400	. . .	. . .	. . .	. . .	. . .	. . .	. . .	. . .
600	. . .	. . .	. . .	. . .	. . .	. . .	. . .	. . .
800	. . .	. . .	. . .	. . .	. . .	. . .	. . .	. . .
1,000	. . .	. . .	. . .	. . .	. . .	. . .	. . .	. . .
1,200	. . .	. . .	. . .	. . .	. . .	. . .	. . .	. . .
1,400	. . .	. . .	. . .	X	X	X	X	X
1,600	X	X	. . .	X	X	X	X	X
1,800	X	X	X	X	X	X	X	X
2,000	X	X	X	X	X	X	X	X

Note: When the first sign of oil droplets wicking up the outer surface of the oil slinger are observed, the parameters are indicated with an X.

Representative pictures are shown in Figs. 6–9 for the disc temperature (80 °C) and pump speed (7.6 ml/min). Figure 6 shows that the lowest disc speed of 200 rpm creates an even, thin film across the surface of the disc.

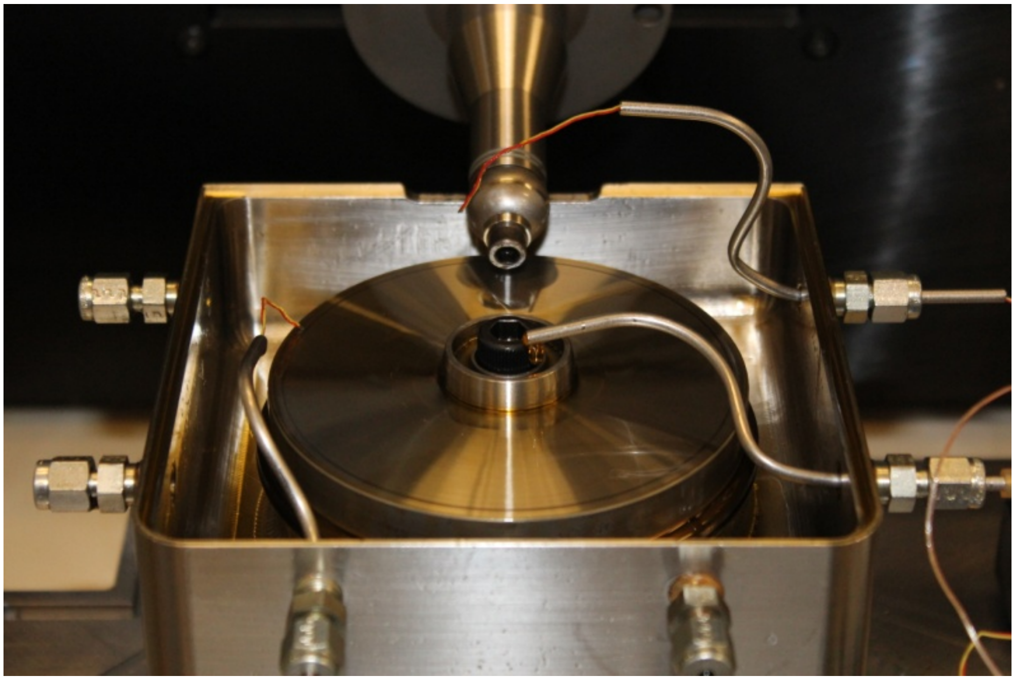

Fig. 6 Disc oil's film at 200 rpm

Figure 7 shows striations beginning to form in the oil film, but all of the oil is remaining attached to the disc.

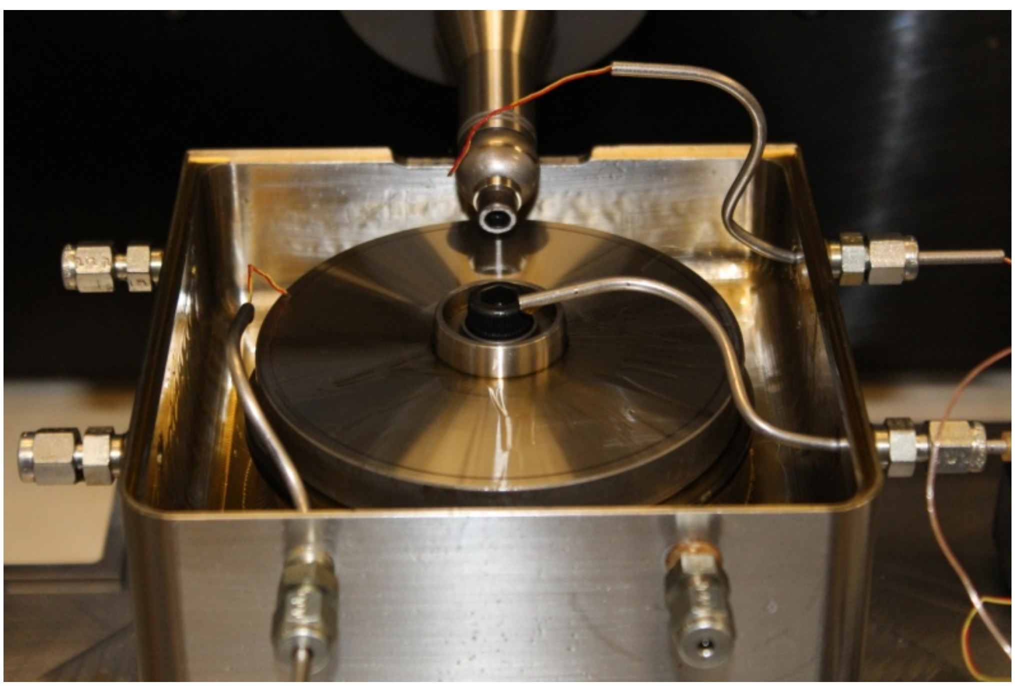

Fig. 7 Disc oil's film at 600 rpm

Figure 8 shows that the oil droplets are beginning to form and detach from the oil slinger at 1,400 rpm. While most of the oil is being transferred to the disc at 1,400 rpm, incomplete delivery of the flow rate is being fed into the experimental contact.

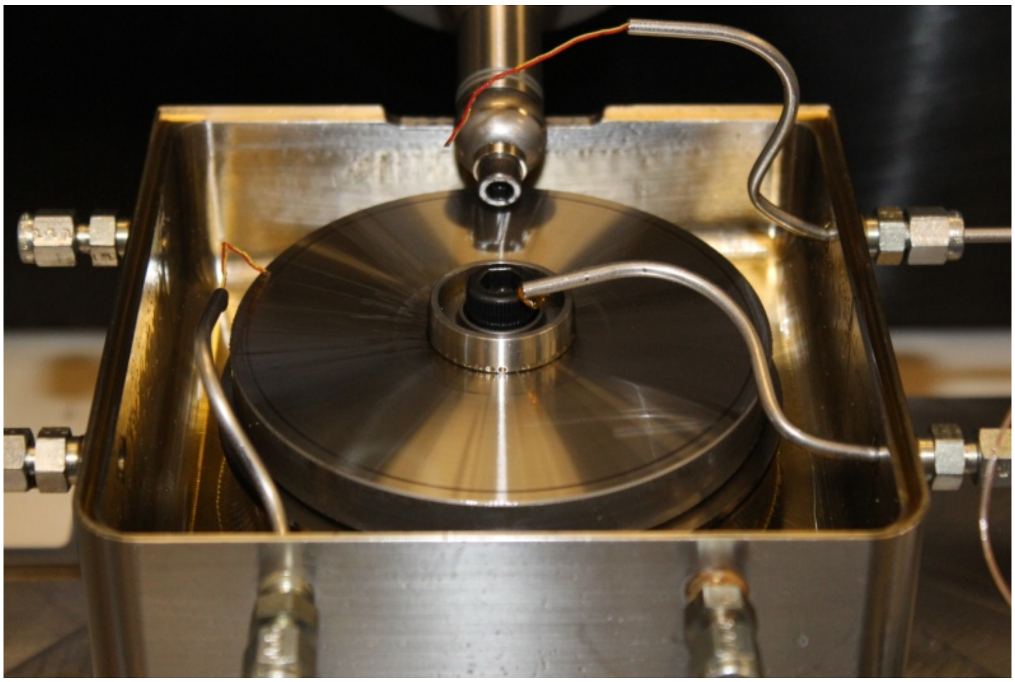

Fig. 8 Disc oil's film at 1,400 rpm

Figure 9 shows all of the oil detaching from the oil slinger (seen as small reflective droplets above the surface of the disc), leaving the disc unlubricated at 2,000 rpm.

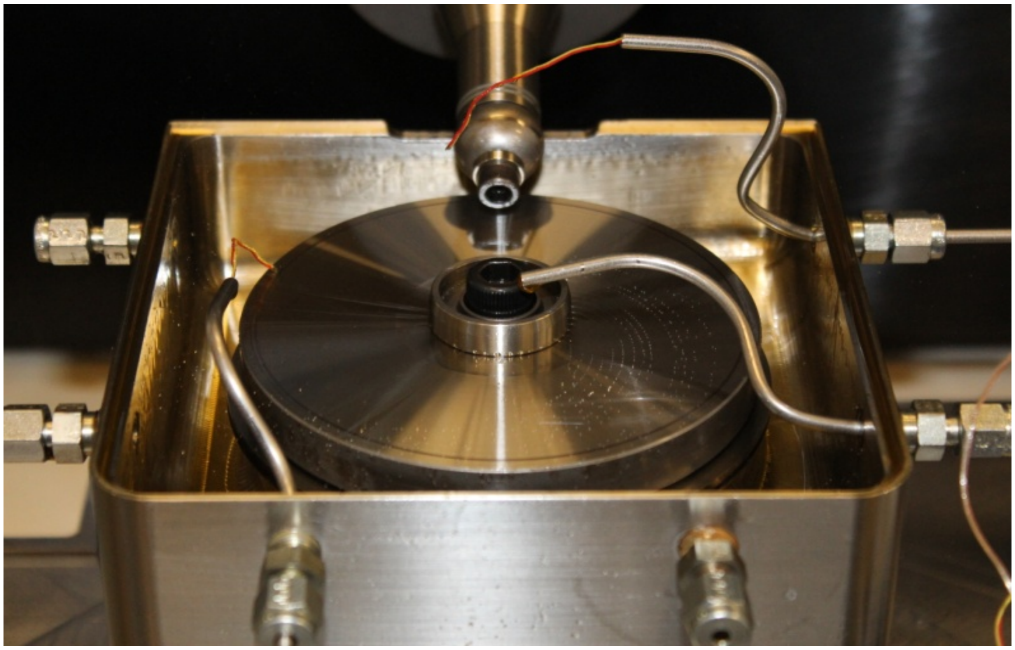

Fig. 9 Disc oil's film at 2,000 rpm

As a result of the oil-slinger analysis, the LC protocol was updated to account for the oil behavior. The LC protocol runs at an entrainment velocity of 16 m/s, which corresponds to disc speeds well above 2,000 rpm. As a result the oil has been fed directly in front of the ball-and-disc contact to create a fully flooded film for all experiments in this report. The complete oil setup with the pass-through oil heater is shown in Fig. 10.

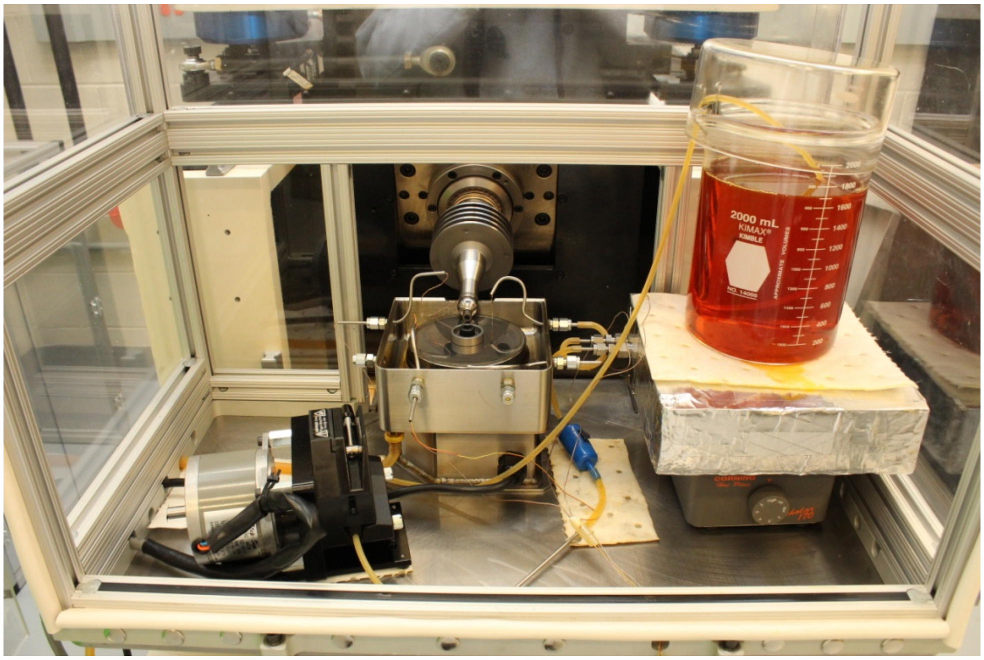

Fig. 10 WAM setup with pass-through oil heater, lid currently removed

2.2.2 Experimentation Results

The results for the LC protocol are given as the load stage where failure is initiated. Failure is indicated by the traction coefficient increasing above 0.15. If failure is not initiated during the experiment, the contact ran through the script successfully and is indicated with the words "run out" in the results. The results for the highest sliding load capacity (HSLC) protocol and the single-tooth load capacity (STLC) protocol are shown in Table 4. Both the basic sequence and the Wedeven protocol's load-stage sequences were used, as discussed earlier. Experiments 205–207 used the basic sequence and Experiment 208 used the Wedeven protocol, which is the standard LC-protocol sequence.

Table 4 LC experimental results

Protocol	Data no.	Material	Surface finish/track history	Oil	Failure load stage (stage no.)	Failure load (N)
STLC	205	9310	As ground	MJII	Run out	NA
HSLC	206		STLC ran out (205)		27	463
HSLC	207		As ground		11	112
STLC	208		As ground		Run out	NA

Figure 11 shows the traction-coefficient plot for each experiment.

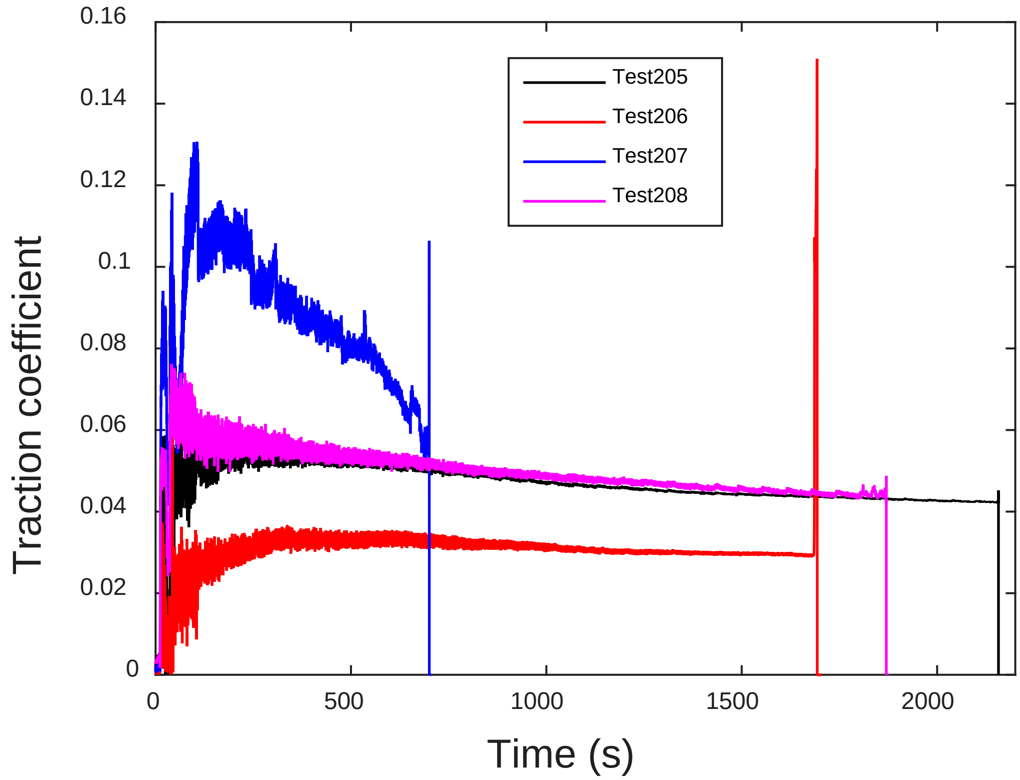

Fig. 11 LC traction-coefficient experimental data

There is a clear disparity between the 2 different relative surface-velocity conditions. The STLC protocol was able to run through its script successfully for both loading sequences with an as-ground surface. The HSLC protocol failed before completion of the loading stages in both cases: early in the load-stage progression at a load of 112 N with an as-ground surface and at a load of 463 N with a smoother, worn-in surface that was polished from the previous STLC experiment, No. 205. It is reasonable to expect this experiment to last longer because its surface asperities were worn away. Presumably, the STLC protocol outperforms the HSLC protocol because of the increased relative sliding velocity of the HSLC protocol. Otherwise the protocols are identical (when the same load-stage sequence is used). Thus, the higher sliding velocity, and corresponding slip percentage, of the HSLC protocol is demonstrated to be more severe than the lower sliding velocity of the STLC protocol.

2.3 LoL Protocol

The LoL protocol has been designed to capture the mechanical behaviors of the gear contact in an LoL condition. In this protocol, one simulates a gear contact at a particular portion of the gear mesh to study the behavior of the lubricant and the material in the contact as the lubricant supply is removed. The primary information gained is the time to the onset of scuffing when the remaining oil film and any lubricating boundary film have broken down. By varying the material, lubricant, finish, and other parameters, their effects can be determined in detail for the chosen position within the gear mesh. Within the protocol, the gear parameters are run for a period of time to reach a quasi-steady-state condition before the oil supply is removed. The time to failure, the main metric of survivability, is indicated by the time from the removal of the oil supply until the traction coefficient increases above 0.15.

2.3.1 Base Protocol

The LoL protocol is run with a constant load, speed, and slip percentage for a set period of time to break in the contacting surface. After this break-in period, the oil supply is shut off and the time to failure is measured. The failure is indicated by a traction coefficient increasing above 0.15, which typically happens quite rapidly and indicates that scuffing has occurred as the lubricant film fails. The results from the LC evaluations identified the most severe condition to be the highest sliding condition. Thus, we selected the high-speed oil-out (HSOO) protocol as the experimental conditions that are most indicative of failure in a gear contact. The parameters are listed in Table 1 with a 10-min break-in period and the same lubrication conditions. The oil supply is then shut off and the contact conditions are held constant until failure is initiated. When failure occurs, the experiment is aborted by removing the load and stopping the motors. The survivability of the contact is measured by the length of time necessary to initiate failure after the oil is shut off.

2.3.2 The Incident–Torque Specifications

An LoL experiment typically experiences harsh conditions and a spike in traction force. If the bolt holding the ball is not tight enough, it may come loose because of the spike in traction force. There were several times the ball bolt was noticeably loose after failure and one such case ultimately led to prolonging the experiment and damaging the machine. The traction-coefficient plot for this incident is shown in Fig. 12. It can be seen that the traction spiked to 0.14, but it did not trigger the shutdown-code limit of 0.15. The ball-spindle bolt was loose for about 6 seconds (s) as it worked its way down into contact with the oil slinger.

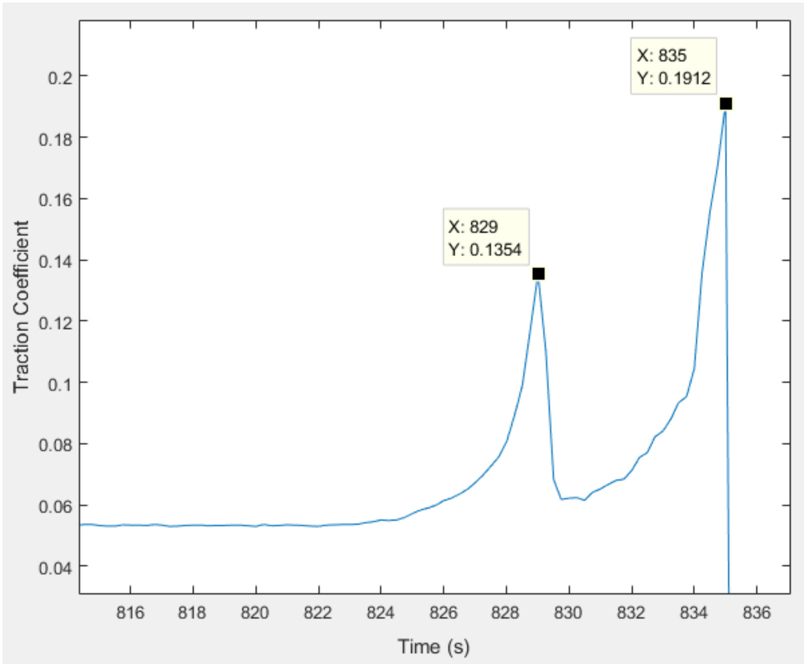

Fig. 12 Traction coefficient of the incident caused by a loose bolt

The 2 rotating surfaces rubbed against each other until the head of the bolt was caught on the top of the oil slinger and broke the screw at its connection to the spindle. With the bolt broken and the WAM attempting to keep the load indicated by the protocol, the ball was pushed out of its track diameter and against the slinger with the edge of the ball spindle's nose piece. The damaged nose piece, screw, and slinger are shown in Fig. 13.

Fig. 13 Damaged parts caused by a loose bolt

The lesson learned from this experience with the LoL protocol is that the ball-and-disc spindles should not be “hand tightened” but torqued down to a specification. The new torque specifications for the bolts are 100–120 in-lb for the ball bolt and 150–200 in-lb for the disc bolt. In addition, the track diameter of 64 mm held the bolt close to the slinger. It is not recommended to run an experiment on a track less than 69 mm to allow for additional clearance between the rotating surfaces.

2.3.3 Evaluation Results

The preliminary HSOO evaluations with 9310 as ground specimens were not able to maintain a nonscuffing contact before the loss of lubrication. This is reasonable because the LC protocol gradually increased the load until failure at 112 N. The HSOO protocol starts with 100 N, so there is no preliminary phase at lower loads where asperities can be removed before the severe condition is applied. While the as-ground specimen failed at a low load (in Table 4), the HSLC experiment run on a polished track—the result of STLC Experiment 205—was able to carry 463 N of load because the asperities were worn away. Thus, a polished surface was observed to have a larger load-carrying capacity. To evaluate polished surfaces, the 9310-steel balls and discs were treated with an isotropic surface finish (ISF) that achieved a 0.051-µm Ra value compared to the 0.17 µm as ground surface. The polished balls and discs were able to withstand the break-in period and produce the time-to-failure results shown in Table 5 along with the traction curves shown in Fig. 14.

Table 5 LoL data with HSOO script

Protocol	Data no.	Material	Surface finish	Oil	Time to failure (s)
	222				145
	422				247
HSOO	423	9310	ISF	MJII	167
	424				83
	425				99

In Fig. 14's traction curves, the oil was shut off at a time of 660 s, after which the traction coefficient is seen to rise from a value of approximately 0.018 to values of 0.025–0.037. The point in time that shows a rapid increase in traction coefficient outside the scale is the initiation of failure.

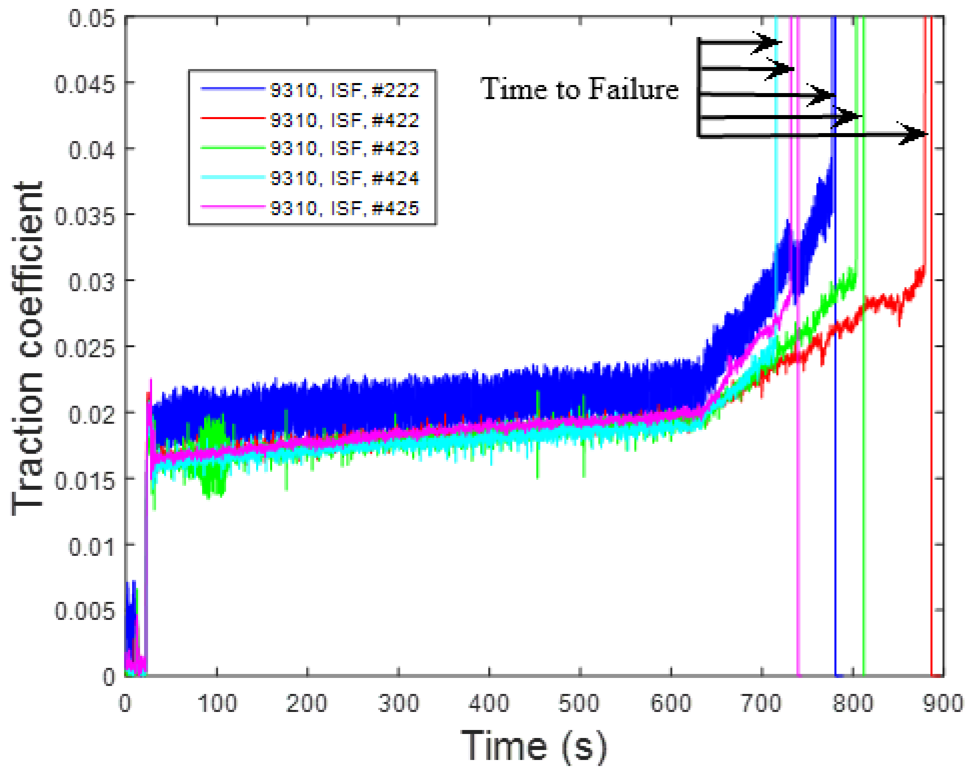

Fig. 14 LoL traction coefficient's time to failure

2.3.4 Oil-Drip Effects

In an LoL experiment it is critical to have a loss of lubricant with zero oil added from the time the oil is shut off until failure. Drops of oil on the disc's or ball's surface help the contact sustain a noticeably longer time to failure than that in a true LoL evaluation.

Two examples of times to failure that were extended because of a drip are HSOO data No. 222 and No. 422 from Table 5. Figure 15 shows that Experiment 222 has a consistent traction coefficient with an increasing trend until it is reduced over a short period of time around 740 s. This is also seen for Experiment 422 with sharp decreases in traction coefficient around 770 s and 850 s of overall run time. These sharp dips in traction coefficient are believed to be the result of oil drips lubricating the surface and allowing it to recover from the verge of failure.

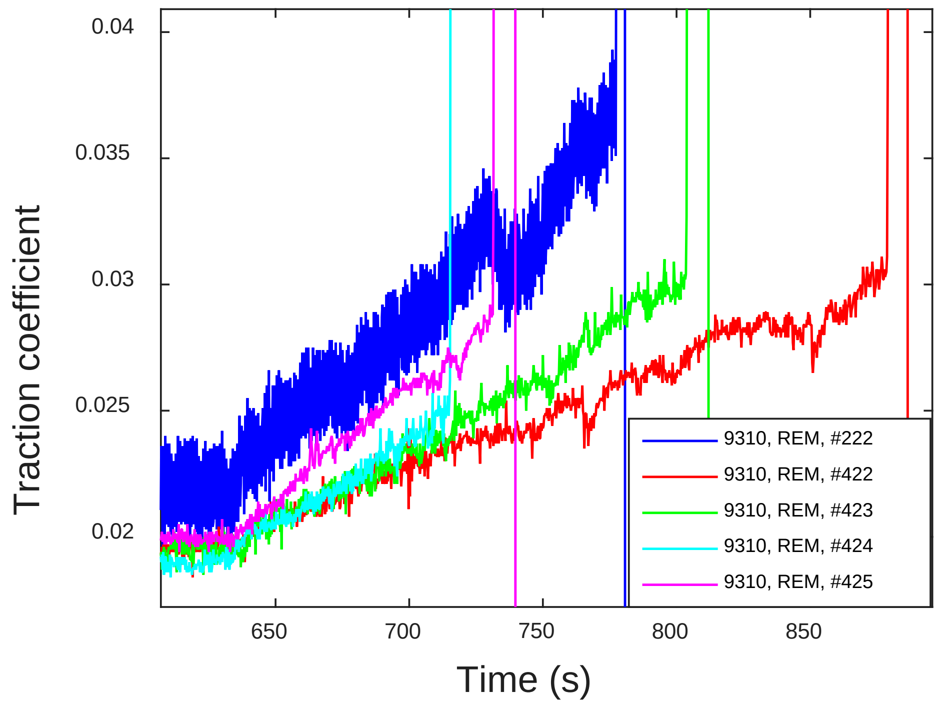

Fig. 15 Zoomed-in LoL data showing decreases in traction due to oil drips

This is especially true with an experiment shown in Fig. 16 that was part of a matrix identifying the effects of materials, surface coatings, and lubricants on the time to failure. The oil was shut off at 660 s, at which point the traction coefficient begins to rise. Several small, rapid decreases in the traction coefficient can be seen that indicate a drip occurred at around 1,300 s, 2,190 s, and 2,275 s on the x-axis. The latter 2 have been expanded in Fig. 17. The experiment in Figs. 16 and 17 lasted 2,274 s after the oil supply was removed, while the average for the particular parameter group, excluding this experiment, was 161 s.

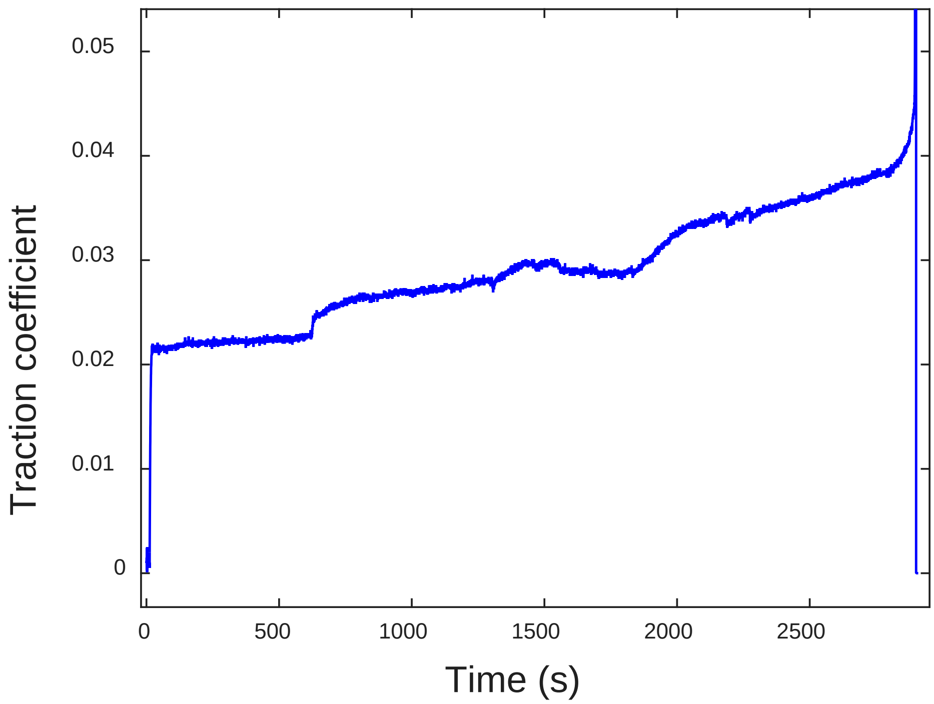

Fig. 16 LoL experiment extended to 2,274 s because of oil drips

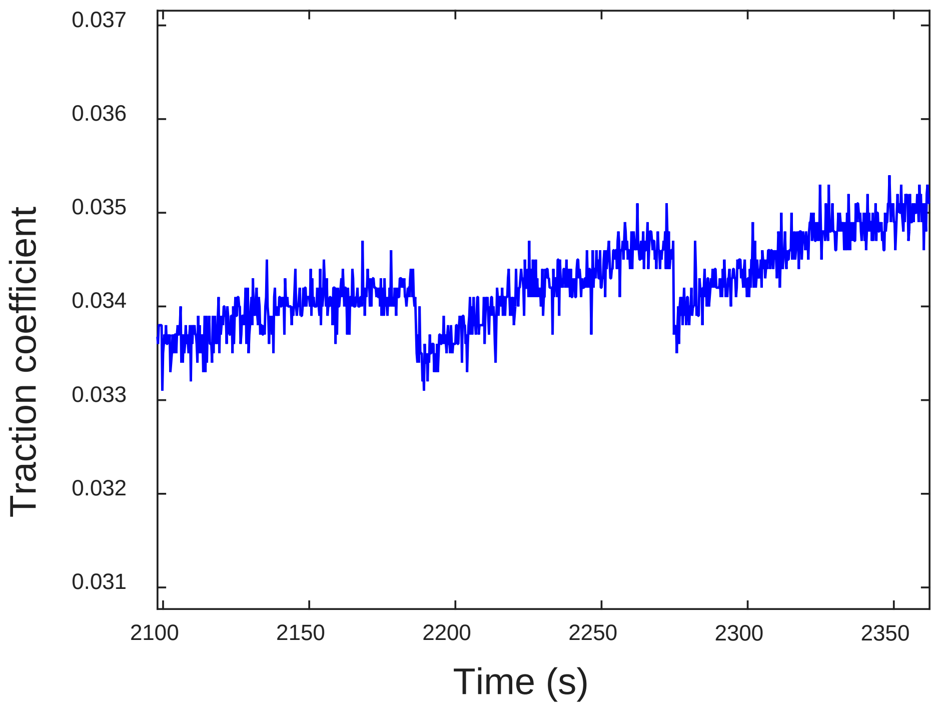

Fig. 17 Close-up examination of 2 of the oil drips in the LoL experiment

Cases in which an oil drip alters the time to failure must be excluded from the average time to failure. The time to failure of the experiment is extended because of the oil drip, but it is also not justifiable to declare the failure to have occurred at the time of the drip or to start the time-to-failure clock again from the drip. If anything can be learned from an experiment with an oil drip it is that the time to failure is somewhere between the time to the first drip and the time to failure of the specimen. This can be a large range and difficult to work with in a statistical analysis because the experiment does not have one defined time-to-failure value.

The formation of oil droplets on the protective covering or the thermocouples and residual oil from the lube pump were all possible sources of oil during experimentation. Several efforts were taken to fully mitigate any source of additional oil in the LoL condition. The most noticeable source of oil accumulation was at the top of the protective covering. To reduce oil drips, an oil pad was used to line the top of the cover, but a simple and reliable means to prevent every drip was not evident. The cover was removed and an oil pad was secured over the top of the ball-and-disc contact to reduce the amount of oil spraying onto the Plexiglas enclosure around the ball-and-disc assembly. The second source of oil came from the disc thermocouple. We determined that we had to run the LoL protocol without a ball thermocouple because of oil wicking onto the track, but the disc thermocouple was also observed to have affected the results. The disc thermocouple was not removed because it is needed to control the heaters as a result of the measured disc temperature. Instead of removing the thermocouple, it was moved from the top surface to the side surface of the disc (as seen in Fig. 18). The last source of oil found within the current setup was from residual oil on the end of the metal tubing used to deliver the oil from the pump. Mitigation was attempted by running the pump backward instead of simply setting the pump speed to zero.

While the excess oil was greatly reduced, some oil could still drip onto the disc. To further reduce the chances of a drip onto the disc, the tubing was positioned outside the radius of the disc (when viewed from above), making residual oil droplets fall outside the disc. The end of the tubing was narrowed and bent toward the disc and the pump rate was increased, causing the oil to squirt diagonally onto the diameter of the track with each pump cycle, as seen in Fig. 18.

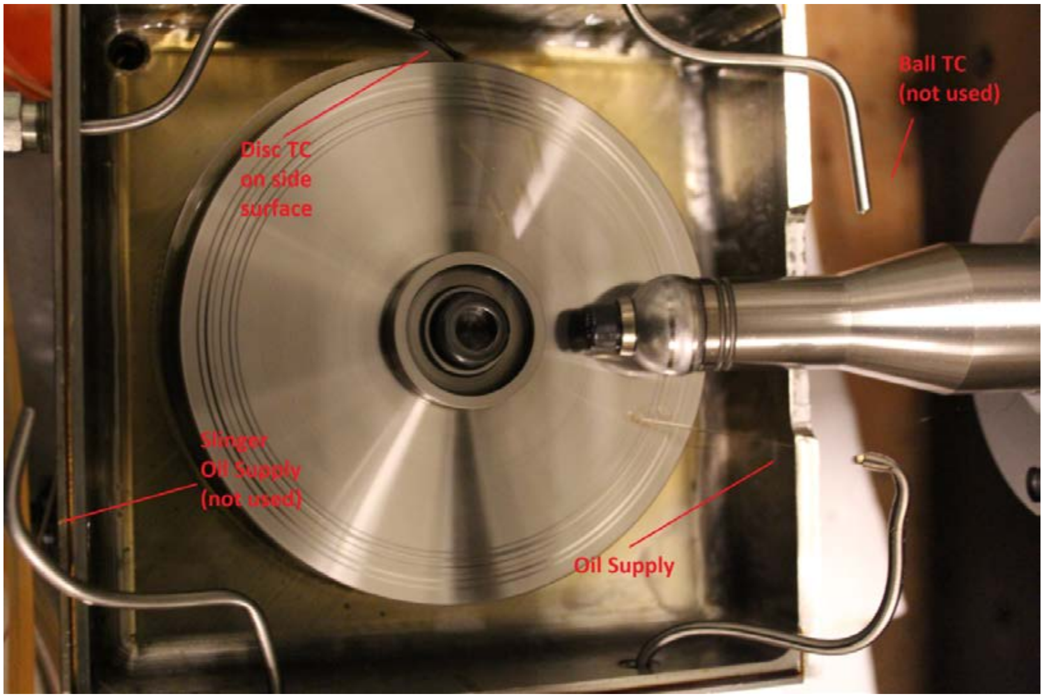

Fig. 18 Final configuration of thermocouples (TCs) and oil supply in LoL experiment

2.3.5 Vibration Effects

The threat of oil drips requires the researcher to scrutinize the entire traction curve—from the time of oil shutoff to time of failure—for irregularities, but this can be very difficult if there is an oscillation in the traction coefficient caused by natural frequencies of the instrument. One example of large oscillations can be seen from data No. 222 in Fig. 14. Despite all of the HSOO experiments having the same set of parameters, there are only oscillations in certain experiments because the change in track diameter between repetitions results in different disc rotational speeds. With each track diameter comes a slightly different set of ball and disc speeds to give the correct combination of entrainment velocity and slip percentage.

This characteristic behavior of the ball-on-disc tribometer was measured over a wide range of ball and disc spindle speeds to understand the source of the extraneous forces. To evaluate a wide range of ball and disc speeds at 16 m/s, the slip percentage was decreased from 150% to 5% slip at intervals of 0.5% slip for 20 s at each slip-percentage interval. All observations were made with the ball and disc out of contact by 0.5 mm with no oil. The traction coefficient is undefined because there is no normal load between the ball and disc. However, the X-Force is used to calculate the traction coefficient with a direct measurement of forces in the direction of the friction force when the ball and disc are operating with parallel velocity vectors. The X-Force data resulted in obvious resonant vibrations, and the root–mean–square (RMS) value of the X-Force was found for each slip percentage's steady-state interval. This RMS value was assigned, respectively, to both ball and disc rotational velocities in Figs. 19 and 20. To determine if the ball or the disc was creating the vibrations, the separate spindles were rotated with the corresponding spindle at 0 rpm. The ball was spun over a range of 0–16,000 rpm at 500-rpm intervals and the disc was spun over a range of 4,000–7,000 rpm at 10-rpm intervals to correspond to the speed ranges captured by the 150% to 5% slip ranges at 16 m/s. The X-Force's RMS for each steady state value was plotted against its respective spindle-speed ranges.

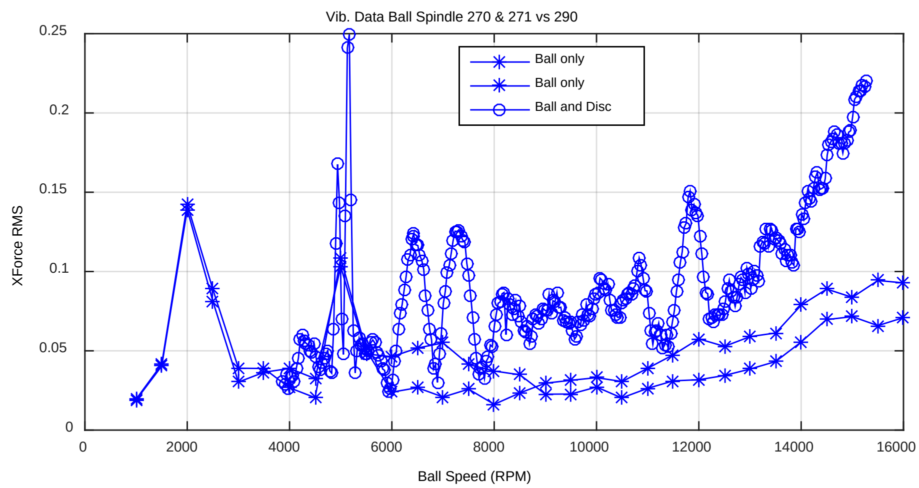

Fig. 19 Ball-spindle effects on the resonant forces

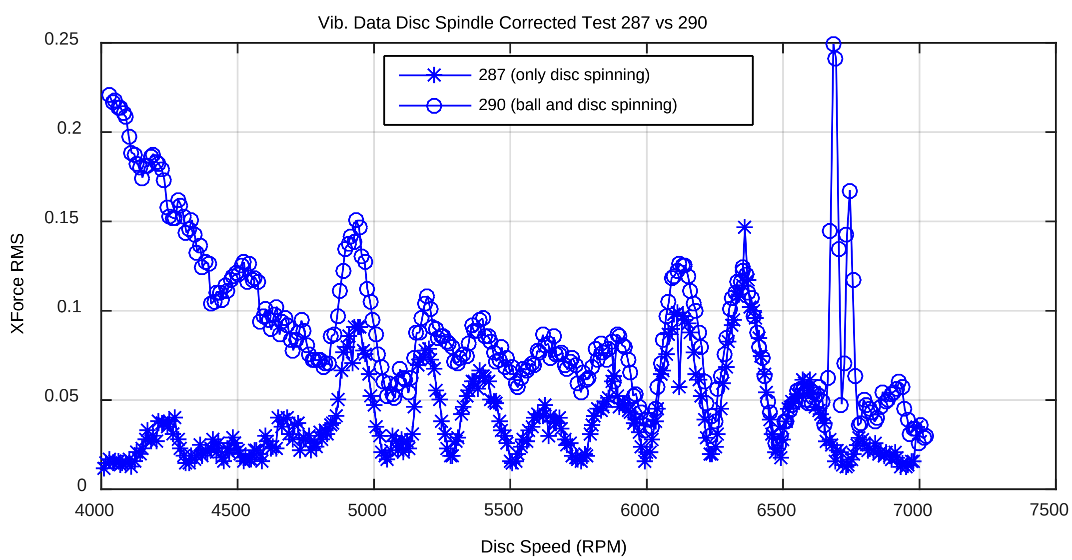

Fig. 20 Disc-spindle effects on the resonant forces

Figures 19 and 20 show that the disc spindle is the source of the irregular forces resulting from resonant frequencies. The ball spindle adds an offset, but the majority of the varying effects are due to the disc. Using this information, the researcher can make small changes to the entrainment velocity during the break-in period to minimize the oscillations while still remaining within a few percent of the experimental parameters and holding a constant sliding velocity between the ball's and disc's surfaces.

3. Summary and Conclusions

A ball-on-disc tribometer is a useful tool with which to research the LoL in a gear or bearing contact to improve survivability. To produce quality data for a rigorous study of individual parameters within the ball-on-disc contact, a well-designed LoL protocol had to be developed. This report laid the foundation for the current LoL protocol by discussing the development of the techniques (and their challenges) and presenting representative data. Variations of and improvements to the LoL protocol will be made in the future to adjust for different gear contacts, lubricant applications, and instrumentation techniques. While changes will be made, the goal of improving the survivability of Army helicopters' power-train components in harsh conditions nevertheless will require carefully developed experimental protocols to properly simulate the contact phenomena.

4. References

1. ADS-50-PRF. Rotorcraft propulsion performance and qualification requirements and guidelines. St. Louis (MO): Army Aviation and Troop Command (US), 1996 Apr 15.

2. Transportation Safety Board of Canada. Main gearbox malfunction/collision with water: Cougar Helicopters Inc., Sikorsky S-92A, C-GZCH, St. John's, Newfoundland and Labrador, 35 nm E, 12 March 2009. Gatineau (QC); 2010 Dec 29. Report No.: A09A0016.

3. Handschuh RF, Polly J, Morales W. Gear mesh loss-of-lubrication experiments and analytical simulation. Cleveland (OH): NASA Glenn Research Center (US): 2011 Nov. Report No.: NASA/TM—2011-217106.

4. Riggs MR, Berkebile SP, Hood AA, Dykas BD. Simulating Army-relevant spur gear contacts with a ball-on-disc tribometer. Aberdeen Proving Ground (MD): Army Research Laboratory (US); 2015 Sep. Report No.: ARL-TR-7492.

5. Wedeven LD, Black WF, Carlisle DJ. Tribology testing of advanced aviation oils, bearing and gear materials. Proceedings of WTC2005, World Tribology Congress III; 2005 Sep 12–16; Washington, DC. ASME; c2005. p. 1,2.

List of Symbols, Abbreviations, and Acronyms

ADS	Aeronautical Design Standard
ARL	US Army Research Laboratory
HS	highest sliding
HSLC	highest sliding load capacity
HSOO	high-speed oil-out
ISF	isotropic surface finish
LC	load capacity
LoL	loss of lubrication
min	minute
MJII	Mobil Jet II
NASA	National Aeronautics and Space Administration
OO	oil-out
RMS	root–mean–square
s	second
ST	single tooth
STLC	single-tooth load capacity
Tb	ball thermocouple
TC	thermocouple
Td	disc thermocouple
Ub	ball linear velocity
Ud	disc linear velocity
Ue	entrainment velocity
WAM	Wedeven Associates Machine

1 (PDF)	DEFENSE TECHNICAL INFORMATION CTR DTIC OCA
2 (PDF)	DIRECTOR US ARMY RESEARCH LAB RDRL CIO LL IMAL HRA MAIL & RECORDS MGMT
1 (PDF)	GOVT PRINTG OFC A MALHOTRA
3 (PDF)	DIR USARL RDRL VTP M RIGGS S BERKEBILE N MURTHY